Supplementary Materials for Underestimation of oceanic carbon uptake in the Arctic Ocean: Ice melt as predictor of the sea ice carbon pump

Benjamin Richaud   Katja Fennel   Eric C.J. Oliver

Michael D. DeGrandpre   Timothée Bourgeois   Xianmin Hu   Youyu Lu

S1   Theoretical Derivation

How does storage of carbon in sea ice impacts the partial pressure of CO_2? To answer this question, one can consider the upper layer of the ocean, partially covered by sea ice forming and melting. The atmospheric pCO_2 and wind speed at 10m height are known, as are the ice concentration and melting-freezing rate and the ocean surface temperature and salinity. The surface ocean pCO_2 (in μatm) would vary along the seasonal cycle due to changes in temperature, salinity, air-sea gas exchange, dilution and concentration related to surface freshwater fluxes (either from precipitation-evaporation, or from ice melt and formation). Biology would also impact carbonate properties due to production and respiration. Finally, advection and mixing could also modify surface properties.

Two scenarios emerge, with for sole difference the storage and release of alkalinity and dissolved inorganic carbon (DIC) by sea ice.

- The first scenario, called CTRL (for control), corresponding to current Earth System Models, does not have any carbon in sea ice. In this case, sea ice melt and formation only dilutes and concentrate carbonate properties in underlying seawater, decreasing or increasing pCO_2 accordingly.

- The second scenario, called EXP (for experiment) corresponding to a more realistic approach, stores some alkalinity and DIC in sea ice. In this case, when ice melts or freezes, on top of diluting or concentrating carbonate properties in underlying waters, it also creates a flux of alkalinity and DIC between ice and ocean. This will further modifies pCO_2 due to chemical equilibration processes.

The difference in pCO_2 between those two scenarios will in turn modify the magnitude of the air-sea gas exchange.

S1.1   Differential Equation

From a mathematical perspective, the difference in pCO_2 between both scenarios would translate as follow. Initial conditions are identical in both scenarios, so $pCO_2^{ICE}(t = 0) = pCO_2^{CTRL}(t = 0)$. If f is the difference in pCO_2 between both runs at each time t, Then:

$$\forall t, \ pCO_2^{ICE}(t) = pCO_2^{CTRL}(t) + \int_0^t f(s)ds$$

If non-linearities are neglected, temperature, salinity and biology changes would impact pCO_2 similarly in both runs. DIC and Alk changes due to dilution and concentration or mixing would have the same impact on pCO_2 in both cases as well. So all those processes can be excluded from f.

The impact of the carbon flux between ice and ocean on pCO_2 needs be taken into account in f. $[Alk]_{ice}$ and $[DIC]_{ice}$ are the alkalinity and DIC concentration inside the sea ice, respectively, in mmol m^{-3} and are assumed to be spatially constant. The flux of alkalinity and DIC between the ice and the ocean is assumed to be directly proportional to the freshwater flux between ice and ocean,

$\mathcal{F}_{FW}^{ice-sea}$, in m s^{-1}. In this case, the ice-ocean flux of alkalinity would be equal to $[Alk]_{ice}\ \mathcal{F}_{FW}^{ice-sea}$, and that of DIC would be $[DIC]_{ice}\ \mathcal{F}_{FW}^{ice-sea}$.

Moreover, this carbon flux, by modifying the surface water pCO_2, would induce a difference in the air-sea gas exchange between both scenarios, written as:

$$\Delta\mathcal{F}_{CO_2}^{air-sea} = \mathcal{F}_{CO_2}^{air-sea,ICE} - \mathcal{F}_{CO_2}^{air-sea,CTRL}$$
$$\Delta\mathcal{F}_{CO_2}^{air-sea} = -k_g(t)S_{CO_2}(t)\lambda(t)\left(pCO_2^{ICE}(t) - pCO_2^{CTRL}(t)\right)$$

where k_g is the gas piston velocity (m s^{-1}), S_{CO_2} is the CO_2 solubility (kg m^{-3} Pa^{-1}) and $\lambda = 1 - [Ice]$ the lead fraction (unitless). The air-sea carbon flux $\Delta\mathcal{F}_{CO_2}^{air-sea}$ and the ice-ocean carbon flux are the only two non-negligible processes that need to be accounted for in f.

Since f corresponds to the change in pCO_2 due to those fluxes, we need to multiply the two different fluxes by the slope of pCO_2 in the alkalinity or DIC domain, $\frac{\partial pCO_2}{\partial Alk}$ and $\frac{\partial pCO_2}{\partial DIC}$. Note that those two terms are fluxes at the surface and therefore have units of μatm m^{-2} s^{-1}. To match the pCO_2 which has units of μatm, we can focus on surface layer of thickness H_0 (m).

Then

$$pCO_2^{ICE}(t) = pCO_2^{CTRL}(t) + \int_0^t \frac{\partial pCO_2}{\partial DIC}\frac{1}{H_0}\Delta\mathcal{F}_{CO_2}^{air-sea}(s)ds$$
$$+ \int_0^t \left(\frac{\partial pCO_2}{\partial Alk}(s)\frac{1}{H_0}[Alk]_{ice}\mathcal{F}_{FW}^{ice-sea}(s) + \frac{\partial pCO_2}{\partial DIC}(s)\frac{1}{H_0}[DIC]_{ice}\mathcal{F}_{FW}^{ice-sea}(s)\right)ds$$

Then, with the notation $g(s) = \frac{\partial pCO_2}{\partial Alk}(s)[Alk]_{ice} + \frac{\partial pCO_2}{\partial DIC}(s)[DIC]_{ice}$ and $\Delta pCO_2^{i-c} = pCO_2^{ICE} - pCO_2^{CTRL}$, we get:

$$\Delta pCO_2^{i-c}(t) = \int_0^t \frac{\partial pCO_2}{\partial DIC}\frac{1}{H_0}\Delta\mathcal{F}_{CO_2}^{air-sea}(s)ds + \int_0^t \frac{1}{H_0}g(s)\mathcal{F}_{FW}^{ice-sea}(s)ds \qquad (1)$$

So, using the gas transfer formulation:

$$\Delta pCO_2^{i-c}(t) = \int_0^t -\frac{\partial pCO_2}{\partial DIC}\frac{1}{H_0}k_g(s)S_{CO_2}(s)\lambda(s)\Delta pCO_2^{i-c}(s)ds + \int_0^t \frac{1}{H_0}g(s)\mathcal{F}_{FW}^{ice-sea}(s)ds$$

While proving the differentiability of all those variables is beyond the scope of this study, it can be noted that they are continuous and unlikely to present any break or cusp. We will therefore assume that we can safely differentiate the previous expression to obtain the following linear differential equation of the first order:

$$\frac{\partial\Delta pCO_2^{i-c}(t)}{\partial t} = -\frac{\partial pCO_2}{\partial DIC}\frac{1}{H_0}k_g(t)S_{CO_2}(t)\lambda(t)\Delta pCO_2^{i-c}(t) + \frac{1}{H_0}g(t)\mathcal{F}_{FW}^{ice-sea}(t) \qquad (2)$$

S1.2 Solving an EDL1

According to the Cauchy-Lipschitz theorem, the Ordinary Differential Equation of order 1 $y' + ay = b$ has a unique general solution (Cauchy, 1844, Chapter 26) of the form:

$$y(t) = e^{-A(t)}\left(K + \int_{t_0}^t b(s)e^{A(s)}ds\right)$$

with $A(t)$ a primitive of $a(t)$ over the proper intervalle and K a constant that depends on initial conditions (at t_0).

So for equation 2, a general solution would be of the form:

$$\Delta pCO_2^{i-c}(t) = e^{-A(t)}\left(K + \int_0^t \frac{1}{H_0}g(s)\mathcal{F}_{FW}^{ice-sea}(s)e^{A(s)}ds\right)$$

with $A(t)$ a primitive of $\frac{\partial pCO_2}{\partial DIC}\frac{1}{H_0}k_g(t)S_{CO_2}(t)\lambda(t)$, written as $A(t) = \int_0^t \frac{\partial pCO_2}{\partial DIC}\frac{1}{H_0}k_g(s)S_{CO_2}(s)\lambda(s)ds + \alpha$.

Since the initial conditions for the control and sensitivity runs are identical, $\Delta pCO_2^{i-c}(t=0) = 0 \Rightarrow K = 0$.

So $\forall t, \Delta pCO_2^{i-c}(t) = e^{-A(t)}\int_0^t \frac{1}{H_0}g(s)\mathcal{F}_{FW}^{ice-sea}(s)e^{A(s)}ds$

S1.3 Uptake difference

Inserting this solution in equation 1 and rearranging, we get:

$$\int_0^t \frac{1}{H_0} \frac{\partial pCO_2}{\partial DIC} \Delta \mathcal{F}_{CO_2}^{air-sea}(s)ds = e^{-A(t)} \int_0^t \frac{1}{H_0} g(s) \mathcal{F}_{FW}^{ice-sea}(s) e^{A(s)} ds - \int_0^t \frac{1}{H_0} g(s) \mathcal{F}_{FW}^{ice-sea}(s)ds$$

If we consider H_0 to be constant, we can move it out of the integrals and make it disappear. Similarly, if $\frac{\partial pCO_2}{\partial DIC}$ is constant and non-null, we can move it outside the integral and divide both side by it.

We can then rearrange as follow:

$$\int_0^t \Delta \mathcal{F}_{CO_2}^{air-sea}(s)ds = \Delta \mathcal{F} = \frac{1}{\frac{\partial pCO_2}{\partial DIC}} \int_0^t g(s) \mathcal{F}_{FW}^{ice-sea}(s) \left(e^{A(s)-A(t)} - 1 \right) ds$$

Note that we can show that if $\lambda(t) = 0$, then $\Delta \mathcal{F}_{CO_2}^{air-sea}(t) = 0$. So we find again the result that the difference in uptake only depends on melting flux (with the assumption that if $[Ice] \neq 1$, ice is melting).

Using realistic alkalinity, DIC and pCO_2 values for the Arctic Ocean ($[Alk]_{sw}$= 2300 mmol m^{-3}, $[DIC]_{sw}$=2100 mmol m^{-3}, $[Alk]_{ice}$= 540 mmol m^{-3}, $[DIC]_{ice}$= 300 mmol m^{-3} and $pCO_2 = 280$ μatm and Revelle and alkalinity factors of 14 and -13.3 respectively), it yields $g(t) \approx -314$ which is negative. All the terms inside the integrand of $A(t) = \int_0^t \frac{\partial pCO_2}{\partial DIC} \frac{1}{H_0} k_g(s) S_{CO_2}(s)\lambda(s)ds + \alpha$ are positive, meaning $A(t)$ is monotonously increasing with t. So $t > s \iff A(t) > A(s)$. This means that $e^{A(t)-A(s)} < 1$. Therefore, the sign of the integrand is determined by the sign of $\mathcal{F}_{FW}^{ice-sea}$.

S1.4 Idealized case

If we make the assumption that wind speed and solubility are constant for the time period when ice is not fully covered the water (i.e. $\forall t$, $\frac{\partial pCO_2}{\partial DIC} \frac{1}{H_0} k_g(t) S_{CO_2}(t) \equiv \kappa$), we can rewrite:

$$
\begin{aligned}
A(t) &= \int_0^t \frac{\partial pCO_2}{\partial DIC} \frac{1}{H_0} k_g(s) S_{CO_2}(s)\lambda(s)ds = \kappa \int_0^t \lambda(s)ds \\
&= \kappa \Lambda(t)
\end{aligned}
$$

with $\Lambda(t) = \int_0^t \lambda(s)ds$. Similarly, we can consider that $\forall t$, $g(t) \equiv \gamma$. Then:

$$\int_0^t \Delta \mathcal{F}_{CO_2}^{air-sea}(s)ds = \frac{1}{\frac{\partial pCO_2}{\partial DIC}} \gamma \int_0^t \mathcal{F}_{FW}^{ice-sea}(s) \left(e^{\kappa(\Lambda(s)-\Lambda(t))} - 1 \right) ds \tag{3}$$

This expression can be evaluated with the ice concentration and the freezing-melting flux used to force the 1D model, described in Section 3.a. To do so, values for γ and κ need to be determined. Using values from Section S1.3, we can set $\gamma = -314$ μatm. Similarly, relying on values from Takahashi et al. [1993], $\frac{\partial pCO_2}{\partial DIC} = 1.9$ μatm mol^{-1} m^3. Following Wanninkhof [2014], their eq. 6, and using an average squared wind speed of 50 m^2 s^{-2} and a surface layer of 1m, we can set $\kappa = 7.7 \times 10^{-4} < U^2 > \frac{\partial pCO_2}{\partial DIC} \frac{1}{H_0} = 7.3 \times 10^{-2}$.

S2 Supplementary Figure
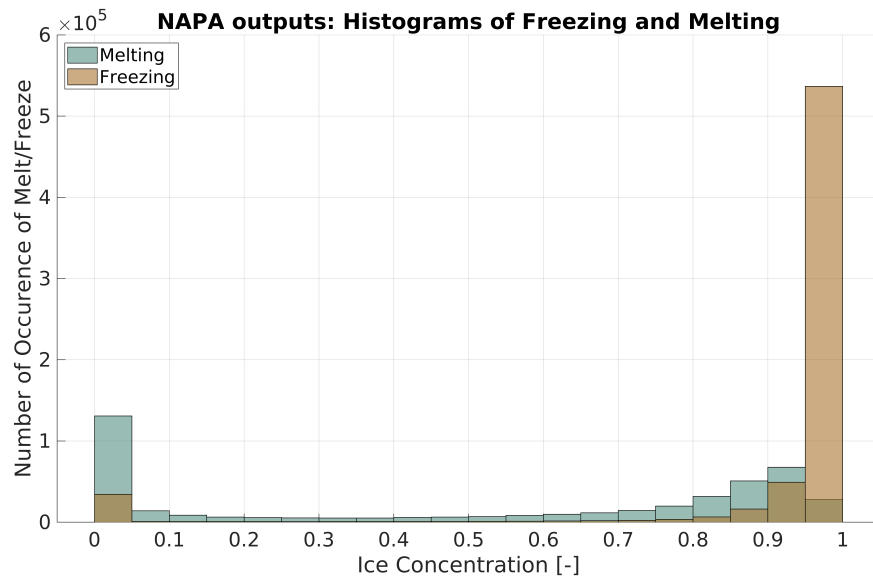
Figure S1: Histograms of freezing and melting as a function of ice concentration. calculated with daily outputs for the NAPA model, from 2014 to 2019, over the 732 grid cells used for the 1D simulation ensemble.
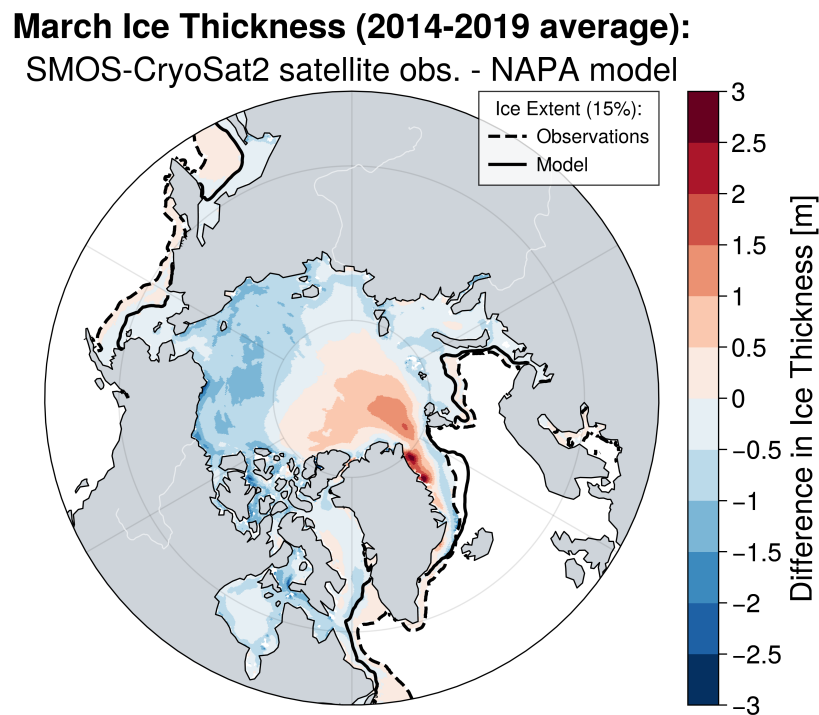
Figure S2: Validation of sea ice concentration: comparison between merged CryoSat2-SMOS satellite observations and NAPA model. Colours show observations minus model ice thickness during the month of maximum extent (March), averaged over 2014-2019. The contours show the ice extent, calculated as the 15% isoline for ice concentration. For details about satellite product, refer to Ricker et al. (2017).
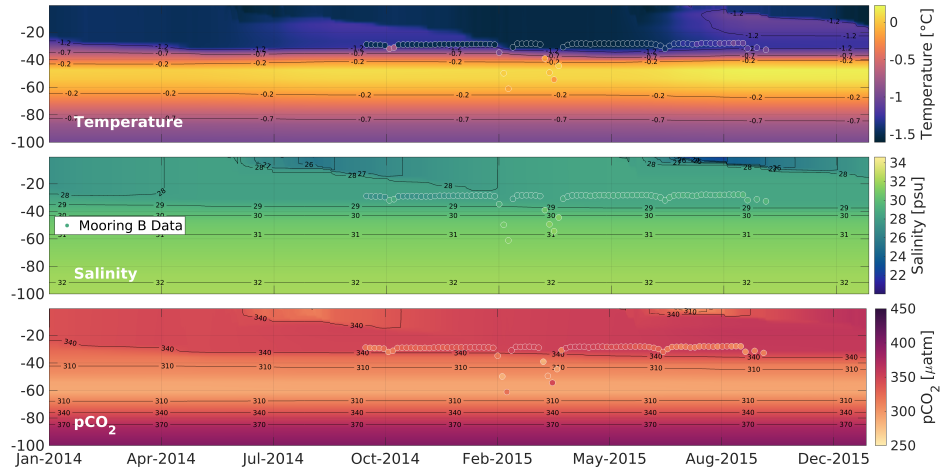
Figure S3: Comparison of 1D numerical model outputs with mooring observations from DeGrandpre et al. (2019) in the Beaufort Gyre station location (78°N, 150°W).

Bibliography

Cauchy, A.-L., Leçons de calcul différentiel et intégral, 1844, 26e leçon.

DeGrandpre, M. D., Lai, C.-Z., Timmermans, M.-L., Krishfield, R. A., Proshutinsky, A., and Torres, D. (2019). Inorganic Carbon and pCO$_2$ Variability During Ice Formation in the Beaufort Gyre of the Canada Basin. Journal of Geophysical Research: Oceans, 124, 4017– 4028. `https://doi.org/10.1029/2019JC015109`

Ricker, R., Hendricks, S., Kaleschke, L., Tian-Kunze, X., King, J., and Haas, C.: A weekly Arctic sea-ice thickness data record from merged CryoSat-2 and SMOS satellite data, The Cryosphere, 11, 1607–1623, `https://doi.org/10.5194/tc-11-1607-2017`, 2017.